

# Transport suppression in heterostructures driven by an ac gate voltage

Miguel Rey <sup>a,\*</sup>, Michael Strass <sup>b</sup>, Sigmund Kohler <sup>b</sup>, Fernando Sols <sup>c</sup>, Peter Hänggi <sup>b</sup>

<sup>a</sup> *Departamento de Física Teórica de la Materia Condensada, Universidad Autónoma de Madrid, E-28049 Madrid, Spain*

<sup>b</sup> *Institut für Physik, Universität Augsburg, Universitätsstraße 1, D-86135 Augsburg, Germany*

<sup>c</sup> *Departamento de Física de Materiales, Universidad Complutense de Madrid, E-28040, Spain*

Received 12 March 2005; accepted 23 March 2005

Available online 23 May 2005

## Abstract

We explore the possibility of inducing in heterostructures driven by an ac gate voltage the coherent current suppression recently found for nanoscale conductors in oscillating fields. The destruction of current is fairly independent of the transport voltage, but can be controlled by the driving amplitude and frequency. Within a tight-binding approximation, we obtain analytical results for the average current in the presence of driving. These results are compared against an exact numerical treatment based on a transfer-matrix approach.

© 2005 Elsevier B.V. All rights reserved.

PACS: 05.60.Gg; 85.65.+h; 72.40.+w

Keywords: Quantum transport; Driven systems; Heterostructures; Tunnelling

## 1. Introduction and modelling

The study of electron transfer comprises a rich variety of systems in many different areas such as chemistry, biology, and life sciences [1,2]. Although electron transfer processes are mainly attributed to electrochemical applications, they are conceptually related to molecular electronics [3–5] and electron transport in low dimensional materials in solid-state physics. In that context, semiconductor heterostructures represent a popular physical system for the investigation of mesoscopic transport [6–8] and tunnelling phenomena [9–13]. The main reason for this is the high mobility and the rather long mean free path of the charge carriers populating them. Standard beam epitaxy techniques make the accurate growth of alloys of such materials on substrates possible, and the

nearly identical lattice parameters, together with the possibility of controlling the band gap, turn the combination GaAs/Al<sub>x</sub>Ga<sub>1-x</sub>As into an ideal candidate for building complex low dimensional structures with quantum wells and tunnel barriers. Moreover, these setups open various ways to study tunnelling in time-dependent systems [14–16]. A straightforward possibility for introducing a time-dependence is the application of an ac transport voltage which only modulates the energies of the electrons in the leads while the potential inside the mesoscopic region remains time-independent. This kind of driving allows for a description within Tien–Gordon theory [17] which expresses the dc current in terms of the static transmission and an effective distribution function for the lead electrons. If the time-dependence enters via an external microwave field or an ac gate voltage, however, such an approach is generally insufficient [18].

A remarkable difference with respect to the static situation is the emergence of inelastic transport channels

\* Corresponding author.

E-mail address: [miguel.rey@uam.es](mailto:miguel.rey@uam.es) (M. Rey).

stemming from the emission or absorption of quanta of the driving field. For a periodically time-dependent transport situation, however, we expect the transmission probabilities and, consequently, the resulting current to be time-dependent as well. This follows indeed from a recently presented Floquet theory for the transport through driven tight-binding systems [16,18]. For the computation of the dc current, this approach justifies the applicability of a Landauer-like current formula where the static transmission is replaced by the time-averaged transmission of the time-dependent system.

The transmission of both the elastic and the inelastic transport channels can depend sensitively on the driving parameters; the contribution of certain channels can even vanish. For the transport across two barriers which enclose an oscillating potential well, Wagner [19] showed that it is possible to suppress the contribution of individual inelastic scattering channels. The total current, however, is given by the sum over all channels, and thus it is not possible to isolate the contribution of a single channel in a current measurement. By contrast, in the case of transport through a two-level system with attached leads, it has been found that driving with a dipole field has directly observable consequences. There, the driving not only affects the contribution of individual transport channels, but the dc current can be suppressed almost entirely [20,21]. Therefore, for the appearance of this *coherent current suppression*, it is essential that the central region consists of at least two weakly coupled wells which oscillate relative to each other [18].

In this work, we explore the possibility of coherent current suppression in double-well heterostructures. Thereby, we compare two theoretical approaches to describe coherent transport in quantum-well structures: The transfer-matrix method and a tight-binding approach. As a model we consider the triple-barrier structure sketched in Fig. 1 where the driving enters via an oscillating gate voltage which modulates the bottom of the left well. The applied transport voltage is assumed to shift the Fermi energy of the left lead by  $-eV$  with

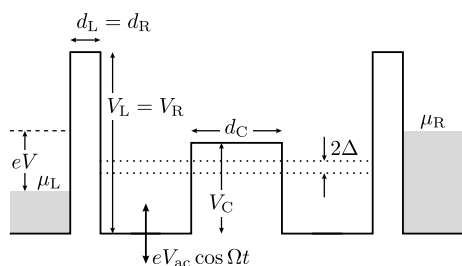


Fig. 1. Model potential for the double-well heterostructure. In the numerical calculations, we employ barriers with the heights  $V_L = V_R = 90$  meV,  $V_C = 40$  meV and the widths  $d_L = d_R = 5$  nm,  $d_C = 15$  nm. The dotted lines mark the energy of a metastable tunnel doublet with splitting energy  $2\Delta$ . The left well is subject to an electric dipole field generated by an alternating gate voltage with amplitude  $V_{ac}$ .

$-e$  being the electron charge. We note that since the time-dependent gate voltage affects only one well, the structure depicted in Fig. 1 is sufficiently asymmetric to also act as an electron pump, i.e., to induce a non-zero current for  $eV = 0$  [16]. In this work, however, we focus on the transport properties in the presence of a finite bias voltage.

For the exact numerical computation of the transmission probabilities, we employ the transfer-matrix method developed by Wagner [22], which is reviewed in Section 2. In Section 3, we introduce the related tight-binding system for which the transport properties can be calculated analytically within a high-frequency approximation scheme [21]. The predictions from the perturbative approach are compared to the exact solution in Section 4.

## 2. Transfer-matrix method

Following Landauer [23], we consider the coherent mesoscopic transport as a quantum mechanical scattering process. The central idea of this approach is the assumption that sufficiently far from the scattering region, the electronic single-particle states are plane waves and that their occupation probability is given by the Fermi function with the chemical potential depending on the applied voltage. The unitarity of evolution under coherent ac driving allows us to write the resulting currents as [24]

$$I = \frac{e}{h} \int dE [T_{RL}(E)f_L(E) - T_{LR}(E)f_R(E)], \quad (1)$$

where  $T_{RL}(E)$  denotes the total transmission probability – i.e., summed over transverse modes and outgoing inelastic channels – of an electron with energy  $E$  from the left lead to the right lead while  $T_{LR}(E)$  describes the respective scattering from the right to the left lead. For time-independent conductors, the time-reversal symmetry of the quantum mechanical scattering process together with the energy conservation ensures  $T_{RL}(E) = T_{LR}(E)$  such that, in the absence of a transport voltage, the current vanishes. This is not the case for a general time-dependent structure [16].

When the total Hamiltonian is time-periodic due to an external driving field,  $H(x, t) = H(x, t + \mathcal{T})$ , one can apply Floquet theory [25,26,14]. It states that the corresponding time-dependent Schrödinger equation has a complete set of solutions of the form

$$\psi_\alpha(x, t) = \exp(-i\epsilon_\alpha t/\hbar)u_\alpha(x, t), \quad (2)$$

where  $u_\alpha(x, t) = u_\alpha(x, t + \mathcal{T})$  denotes the so-called Floquet states, and  $\epsilon_\alpha$  the so-called quasienergies in analogy to the quasimomenta of Bloch theory.

Owing to their time-periodicity, we can decompose the Floquet states into a Fourier series

$$u_x(x, t) = \sum_{n=-\infty}^{\infty} e^{-in\Omega t} u_{x,n}(x). \quad (3)$$

The form (3) of the Floquet states suggests that during the scattering, an electron with initial energy  $E$  evolves into a *coherent* superposition of states with energies  $E' = E + n\hbar\Omega$ . The arbitrary integer  $n$  is referred to as the sideband index; the inelastic channels are called sidebands. We emphasise that, despite the existence of a band bottom, the summation over  $n$  in Eq. (3) is unrestricted.

A proper calculation of the dc current through a time-dependent scatterer must now include these inelastic channels, and the Landauer formula of Eq. (1) has to be conveniently generalised to take them into account. Since the Floquet scattering states can be thought of as having been created from the orthogonal dc states by adiabatically switching on the driving, they too must be orthogonal, so that it is sufficient to sum over channels incident from both leads [24].

In the transfer-matrix method described below, the Floquet states are decomposed into plane waves throughout the driven heterostructure, so that they can be appropriately matched with the scattering channels in the leads. This decomposition allows us to separate the time- and the space-dependent parts of the wave function, thus obtaining directly the time-independent probabilities that go into Eq. (1).

For a spatially constant potential with a time-dependent gate voltage  $V_{ac}(t)$ , the solution of the Schrödinger equation is readily obtained to read

$$\psi(E, z, t) = \sum_{n=-\infty}^{+\infty} \psi_n(z) \exp \left\{ -\frac{i}{\hbar} (E + n\hbar\Omega)t - i\phi(t) \right\} \quad (4)$$

with the accumulated phase

$$\phi(t) = \frac{e}{\hbar} \int^t dt' V_{ac}(t') = \phi(t + \mathcal{T}). \quad (5)$$

Its time-periodicity follows from the zero time-average of the gate voltage.

Neighbouring layers of a heterostructure may have different ac voltages applied in addition to different band-edges. As a consequence, the wave functions in Eq. (4) which solve the Schrödinger equation in each layer do not coincide in the general case. The solution for the complete system has to be constructed by matching the corresponding wave functions at the interfaces between layers. With this goal in mind, we assume that the wave function (4) is a solution of the Schrödinger equation for the time-dependent Hamiltonian

$$\begin{aligned} H(z, t) &= H_0(z) + eV_{ac}(t) \\ &= -\frac{\hbar^2}{2} \frac{\partial}{\partial z} \frac{1}{m(z)} \frac{\partial}{\partial z} + V(z) + eV_{ac} \cos \Omega t, \end{aligned} \quad (6)$$

and that, moreover,  $\psi_n(z)$  is an eigenfunction of the time-independent Hamiltonian  $H_0$  with the spatially piecewise constant effective mass  $m(z)$ , and has the general form

$$\psi_n(z) = A_n \exp(k_n z) + B_n \exp(-k_n z). \quad (7)$$

The wave vector

$$k_n = [2m(V - E - n\hbar\Omega)]^{1/2} \quad (8)$$

describes travelling as well as decaying waves (bound states) for complex and real values of  $k_n$ , respectively. The matching conditions at an interface follow from the fact that both the wave function and the flux have to be continuous, i.e., at  $z = z_0$

$$\begin{aligned} \lim_{z \rightarrow z_0^+} \psi(z, t) &= \lim_{z \rightarrow z_0^-} \psi(z, t), \\ \lim_{z \rightarrow z_0^+} \frac{1}{m(z)} \frac{\partial}{\partial z} \psi(z, t) &= \lim_{z \rightarrow z_0^-} \frac{1}{m(z)} \frac{\partial}{\partial z} \psi(z, t). \end{aligned} \quad (9)$$

This yields an infinite system of algebraic equations for the coefficients  $A_n$  and  $B_n$  in each layer. Inserting the Fourier expansion of the phase in Eq. (5),

$$\exp \left\{ -\frac{ie}{\hbar\Omega} V_{ac} \sin \Omega t \right\} = \sum_{n'=-\infty}^{+\infty} J_{n'} \left( \frac{eV_{ac}}{\hbar\Omega} \right) \exp(-in'\Omega t), \quad (10)$$

where  $J_{n'}$  is the  $n'$ 'th order Bessel function of the first kind, allows one to recast these equations for an interface between layers I and II at  $z = z_i$  in matrix form:

$$\mathbf{T}_{z_i}^I \begin{pmatrix} A_n^I \\ B_n^I \end{pmatrix} = \mathbf{T}_{z_i}^{II} \begin{pmatrix} A_n^{II} \\ B_n^{II} \end{pmatrix}. \quad (11)$$

The matrices  $\mathbf{T}_{z_i}^I$  and  $\mathbf{T}_{z_i}^{II}$  with elements  $T_{z_i;n,n'}^I$  and  $T_{z_i;n,n'}^{II}$ , respectively, are of infinite dimension, and contain the coefficients of all possible scattering channels, i.e., photon exchanges between the incoming electron and the driving field, at either side of the interface. Their precise form depends on whether or not a layer is affected by the time-dependent gate voltage. The transfer matrix  $\mathbf{T}_{z_i \rightarrow z_j}$  between two sides of a layer of width  $z_j - z_i$  is then defined as [27]

$$\mathbf{T}_{z_i \rightarrow z_j} = \mathbf{T}_{z_j}^I (\mathbf{T}_{z_i}^I)^{-1}. \quad (12)$$

This definition in terms of layers, rather than using a similar one across interfaces, is physically more sensible, since the matrices depend on the properties of just one layer. They are also numerically easier to implement, as there are fewer qualitatively different matrices to deal with. To calculate the total transfer matrix across the structure, we have to multiply the matrices across all different layers and obtain

$$\mathbf{T}_{L \rightarrow R} = \mathbf{T}_{z_R} \mathbf{T}_{z_j \rightarrow z_R} \cdots \mathbf{T}_{z_L \rightarrow z_j} \mathbf{T}_{z_L}, \quad (13)$$

where  $\mathbf{T}_{z_L}$  and  $\mathbf{T}_{z_R}$  represent the initial and final matrices at the ends of the heterostructure. With the elements  $T_{L \rightarrow R}^{n,n'}$  of the total transfer matrix we can find the probability that an electron with energy  $E + n\hbar\Omega$  in lead L is scattered into a channel with energy  $E' = E + n'\hbar\Omega$  in lead R, with integer  $n, n'$ . The diagonal elements  $T_{L \rightarrow R}^{n,n}$  are closely related to the (static) transmission probability  $T_{RL}$ , while the off-diagonal elements  $T_{L \rightarrow R}^{n \neq n'}$  describe the effects of the absorption or emission of  $n - n'$  photons on the transmission probability of the electron. For flat conduction bands on both sides of the heterostructure, the wave functions in the contacts are plane waves, and in this case the proper boundary conditions to describe an electron incident from, say, the left-hand side at energy  $E$  are  $A_L^n = \delta_{n,0}$  and  $B_R^n = 0$ . The transmission probability in sideband  $n$  is then defined as

$$T_{RL}^n = \frac{k_R^n}{k_L^n} \frac{m_L}{m_R} \left| \frac{A_R^n}{A_L^0} \right|^2, \quad (14)$$

where  $k_R^n$  and  $k_L^0$  represent the wave vectors on the right- and left-hand side in sidebands  $n$  and 0, respectively.

In a numerical implementation of the transfer-matrix technique, it is necessary to truncate the infinite matrices. Thereby for consistency, a proper cut-off has to be so large that unitarity of the scattering process is preserved, i.e.,

$$\sum_{n=-\infty}^{+\infty} T_{RL}^n + \sum_{n=-\infty}^{+\infty} R_{LL}^n = 1, \quad (15)$$

where  $R_{LL}^n$  represents the reflection probability of an electron to be reflected from energy  $E$  into a sideband at energy  $E + n\hbar\Omega$  on the same side. The number of sidebands that need to be taken into account to meet a given accuracy (which in our calculations was set to  $10^{-17}$ ) depends essentially on the ratio  $eV_{ac}/\hbar\Omega$ , as this is the argument of the Bessel function  $J_n$  that determines the weight of each sideband  $n$ . To proceed, one starts at the initial value of  $V_{ac} = 0$  with a tentative number of sidebands, and increases it for growing driving amplitudes if a check with Eq. (15) suggests that unitarity is breaking down. When particle number conservation is restored one can go to a higher  $V_{ac}$ . Transfer matrices such as those employed here have the advantage of being easily scalable to arbitrarily complex structures. The combination of flexibility in structural properties and numerical accuracy makes this method well-suited to the study of strongly driven semiconductor heterostructures.

### 3. Tight-binding approximation

A different approach to study resonant tunnelling in a driven double-well structure is based on the adoption of a tight-binding (TB) picture. Fig. 2 depicts the TB

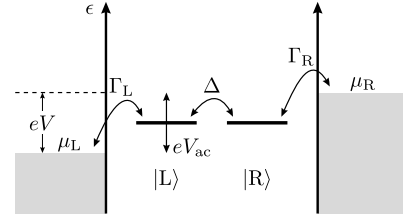


Fig. 2. Schematic energy diagram of a symmetric double-well structure in the tight-binding approximation. The tunnelling matrix element is given by  $\Delta$  and each well couples with  $\Gamma_L$  and  $\Gamma_R$  to the associated lead. The state  $|L\rangle$  in the left well is driven by an oscillating gate voltage with amplitude  $V_{ac}$ . In addition, an external bias  $V = (\mu_R - \mu_L)/e$  is applied.

configuration corresponding to the heterostructure introduced above.

#### 3.1. The model

Then, the Hamiltonian of the system is given by

$$H(t) = H_{\text{wells}}(t) + H_{\text{leads}} + H_{\text{contacts}}, \quad (16)$$

where the individual terms describe the driven quantum wells, the electron reservoirs in the leads, and the coupling of the left and the right well to the respective neighbouring lead. For simplicity, we neglect the electron spin.

Within the framework of the TB approximation, the time-dependent quantum-well Hamiltonian reads

$$\begin{aligned} H_{\text{wells}}(t) &= \sum_{\ell, \ell'} H_{\ell, \ell'}(t) c_{\ell}^{\dagger} c_{\ell'} \\ &= -\Delta (c_L^{\dagger} c_R + c_R^{\dagger} c_L) + eV_{ac} \cos(\Omega t) c_L^{\dagger} c_L. \end{aligned} \quad (17)$$

An electron can be localised in the left or right well, whereupon the fermion operator  $c_{\ell}$  ( $c_{\ell}^{\dagger}$ ) annihilates (creates) an electron in the respective well ( $\ell = L, R$ ). These localised states  $|L\rangle$  and  $|R\rangle$  are coupled by the tunnelling matrix element  $\Delta$ . For convenience, the energy scale is set such that the on-site energies of the two resonant TB levels are zero and lie exactly halfway in between the transport bias window defined by the chemical potentials  $\mu_L$  and  $\mu_R$ . The second term of the Hamiltonian (17) accounts for the harmonic driving of the traversing electrons in the left well via an oscillating gate voltage with amplitude  $V_{ac}$  and period  $\mathcal{T} = 2\pi/\Omega$ .

The leads are modelled as ideal Fermi gases with the Hamiltonian

$$H_{\text{leads}} = \sum_{\ell, q} \epsilon_{\ell q} c_{\ell q}^{\dagger} c_{\ell q}, \quad (18)$$

where  $c_{\ell q}$  ( $c_{\ell q}^{\dagger}$ ) annihilates (creates) an electron in the lead with energy  $\epsilon_{\ell q}$  with  $\ell = L, R$ . As an initial condition, we employ the grand-canonical ensembles of electrons in the leads at inverse temperature  $\beta = 1/k_B T$ . Therefore, the lead electrons are characterised by the equilibrium Fermi distribution  $f_{\ell}(\epsilon_{\ell q}) = \{1 + \exp[-\beta(\epsilon_{\ell q} - \mu_{\ell})]\}^{-1}$ .

The localised state in each well couples via the tunnelling matrix element  $V_{\ell q}$  to the state  $|\ell q\rangle$  in the respective lead. The Hamiltonian which describes this interaction has the form

$$H_{\text{contacts}} = \sum_{\ell, q} V_{\ell q} c_{\ell q}^\dagger c_\ell + \text{H.c.} \quad (19)$$

The lead–well coupling is entirely specified by the spectral density  $\Gamma_\ell(\epsilon) = 2\pi \sum_q |V_{\ell q}|^2 \delta(\epsilon - \epsilon_{\ell q})$ . Since, for the system at hand, the bandwidth of the conduction band of the leads is much larger than the energy regime where transport happens, the spectral densities are practically constant, i.e.,  $\Gamma_\ell(\epsilon) = \Gamma_\ell$ , which defines the so-called wide-band limit.

### 3.2. Floquet transport theory

In order to determine the time-averaged dc current which matches Eq. (1) for the TB approximation, we employ a generalised Floquet approach to solve the corresponding Heisenberg equations of motion and derive an expression for the retarded Green's function in terms of Floquet states. This result is applied to study transport by evaluating the operator  $I_\ell(t) = ie[H(t), \sum_q c_{\ell q}^\dagger c_{\ell q}]$  for the time-dependent current through contact  $\ell$ . In the next subsection we will also derive an analytic expression for the current valid in the high frequency limit with respect to the driving.

We start out by stating the solution of the Heisenberg equations of motion for the lead operators, which is given for the left lead by [18]

$$c_{Lq}(t) = c_{Lq}(t_0) e^{-i\epsilon_{Lq}(t-t_0)/\hbar} - \frac{iV_{Lq}}{\hbar} \int_{t_0}^t dt' e^{-i\epsilon_{Lq}(t-t')/\hbar} c_L(t'). \quad (20)$$

For the corresponding solution of  $c_{Rq}(t)$ , L has to be substituted by R. Now inserting these solutions into the Heisenberg equations of motion for the quantum wells yields the two coupled linear differential equations

$$\dot{c}_L = -\frac{ie}{\hbar} V_{ac} \cos(\Omega t) c_L - \frac{\Gamma_L}{2\hbar} c_L + \frac{i}{\hbar} \Delta c_R + \zeta_L(t), \quad (21)$$

$$\dot{c}_R = \frac{i}{\hbar} \Delta c_L - \frac{\Gamma_R}{2\hbar} c_R + \zeta_R(t). \quad (22)$$

Here, within the wide-band limit, the coupling to the leads has been eliminated in favour of the spectral density  $\Gamma_\ell$  and the fermionic fluctuation operator

$$\zeta_\ell(t) = -\frac{i}{\hbar} \sum_q V_{\ell q}^* e^{-i\epsilon_{\ell q}(t-t_0)/\hbar} c_{\ell q}(t_0). \quad (23)$$

Assuming that the initial conditions are those of the grand canonical ensemble, this Gaussian noise operator satisfies

$$\langle \zeta_\ell(t) \rangle = 0, \quad (24)$$

$$\langle \zeta_\ell^\dagger(t) \zeta_{\ell'}(t') \rangle = \delta_{\ell\ell'} \frac{\Gamma_\ell}{2\pi\hbar^2} \int d\epsilon e^{i\epsilon(t-t')/\hbar} f_\ell(\epsilon). \quad (25)$$

Then the operator for the time-dependent current through the left lead becomes [18]

$$I_L(t) = \frac{e\Gamma_L}{\hbar} c_L^\dagger(t) c_L(t) - e[c_L^\dagger(t) \zeta_L(t) + \zeta_L^\dagger(t) c_L(t)] \quad (26)$$

with a corresponding expression for  $I_R(t)$ . Here we made use of the wide-band limit. To evaluate the time-dependent current, we thus have to find the solution for the inhomogeneous set of the quantum Langevin equations (21) and (22) of the quantum-well operators, which is formally given by

$$c_\ell(t) = \int_0^\infty d\tau [G_{\ell L}(t, t-\tau) \zeta_L(t-\tau) + G_{\ell R}(t, t-\tau) \zeta_R(t-\tau)] \quad (27)$$

in the stationary limit  $t_0 \rightarrow \infty$  with  $\ell = L, R$ . What remains is to determine the retarded Green's function  $G(t, t-\tau)$ . This is where Floquet theory comes into play by making use of the  $\mathcal{T}$ -periodicity of the driving. Solving the Floquet eigenvalue equation

$$\left( \mathcal{H}_{\text{wells}}(t) - i\Sigma - i\hbar \frac{\partial}{\partial t} \right) |u_\alpha(t)\rangle = (\epsilon_\alpha - i\hbar\gamma_\alpha) |u_\alpha(t)\rangle \quad (28)$$

of the physical problem at hand, where  $\mathcal{H}(t) = \sum_{\ell, \ell'} |\ell\rangle H_{\ell, \ell'}(t) \langle \ell'|$ , we get the Floquet states  $|u_\alpha(t)\rangle$  and the complex-valued quasienergies  $\epsilon_\alpha - i\hbar\gamma_\alpha$ . Note that the prior equation is, in contrast to the usual Floquet equation, non-Hermitian. This is due to the presence of the self-energy  $2\Sigma = |L\rangle \Gamma_L \langle L| + |R\rangle \Gamma_R \langle R|$ , which results from tracing out the leads [28]. Therefore, Eq. (28) has to be solved also for its adjoint eigenstates  $|u_\alpha^\dagger(t)\rangle$  [16]. With the corresponding expression for the propagator  $U(t, t-\tau)$ , the retarded Green's function assumes the form

$$G(t, t-\tau) = \sum_\alpha e^{-i(\epsilon_\alpha/\hbar - i\gamma_\alpha)\tau} |u_\alpha(t)\rangle \langle u_\alpha^\dagger(t-\tau)| \Theta(\tau), \quad (29)$$

where  $\Theta(\tau)$  is the Heaviside step function.

The dc current is now obtained by calculating the expectation value  $\langle I_L(t) \rangle$  and averaging over one driving period. This time-averaging will cancel those terms of  $\langle I_L(t) \rangle$ , which are responsible for a  $\mathcal{T}$ -periodic charging of the wire. After eliminating backscattering terms [18], we arrive at the very compact form for the final result

$$\bar{I} = \frac{e}{\hbar} \sum_n \int d\epsilon \left[ T_{LR}^{(n)}(\epsilon) f_R(\epsilon) - T_{RL}^{(n)}(\epsilon) f_L(\epsilon) \right], \quad (30)$$

where the total transmission probabilities are given by  $T_{LR}^{(n)}(\epsilon) = \Gamma_L \Gamma_R |G_{LR}^{(n)}(\epsilon)|^2$  and  $T_{RL}^{(n)}(\epsilon) = \Gamma_L \Gamma_R |G_{RL}^{(n)}(\epsilon)|^2$ , which resemble the Fisher–Lee relation [29]. The above equation also holds for the current through the right contact owing to charge conservation. The Green's function

$$G^{(n)}(\epsilon) = \sum_{\alpha, n'} \frac{|u_{\alpha, n'+n}\rangle \langle u_{\alpha, n'}^\dagger|}{\epsilon - (\epsilon_\alpha + n'\hbar\Omega - i\hbar\gamma_\alpha)} \quad (31)$$

is the  $t$ -averaged Fourier transformed of the propagator (29). Physically, it describes the propagation of a transmitted electron with initial energy  $\epsilon$  from one lead to the other lead undergoing scattering events with emission ( $n < 0$ ) or absorption ( $n > 0$ ) of  $|n|$  photons, or being transmitted elastically ( $n = 0$ ).

### 3.3. High-frequency limit

The Floquet treatment of the present transport problem allows for the implementation of a stationary perturbation scheme for driving frequencies much larger than all other frequency scales of the system [26]. This approach has recently been extended to transport situations which are characterised by the presence of leads [18,21]; here we only outline the derivation and refer the reader to [16]. A particular benefit of this perturbation scheme is the achievement of a physical understanding of the transport processes by approximately mapping the time-dependent problem to a static one with renormalised parameters. For the static situation, in turn, the current is well known by Eq. (1), where the transmission in the wide-band limit reads  $T(\epsilon) = T_{LR}(\epsilon) = \Gamma_L \Gamma_R |G_{LR}(\epsilon)|^2$ . This looks similar to the driven case but with  $n = 0$  and therefore we have in contrast to the driven system  $G_{LR}(\epsilon) = G_{RL}(\epsilon)$ . For the static system given by (16) with  $V_{ac} = 0$ , we obtain for the transmission

$$T(\epsilon) = \frac{\Gamma^2 \Delta^2}{|(\epsilon - i\Gamma/2)^2 - \Delta^2|^2} \quad (32)$$

assuming equal coupling to the leads ( $\Gamma_\ell = \Gamma$ ).

The starting point of the approximation scheme is the unitary transformation

$$U_0(t) = \exp \left\{ -\frac{ie}{\hbar\Omega} V_{ac} \sin(\Omega t) c_L^\dagger c_L \right\}, \quad (33)$$

which is first applied to the quantum-well Hamiltonian (17). For sufficiently large driving frequencies  $\Omega \gg \Delta/\hbar$ , a separation of time scales is performed by this transformation. Thereby, fast oscillations of the transformed Hamiltonian are neglected by averaging over a driving period [14,30]. Finally, we arrive at the effective Hamiltonian for the quantum wells

$$\begin{aligned} \bar{H}_{\text{eff}} &= \frac{1}{\mathcal{T}} \int_0^{\mathcal{T}} dt (U_0^\dagger H_{\text{wells}}(t) U_0 - i\hbar U_0^\dagger \dot{U}_0) \\ &= -\Delta_{\text{eff}} (c_L^\dagger c_R + c_R^\dagger c_L), \end{aligned} \quad (34)$$

which is of the same form as in the static case but with the effective tunnelling matrix element  $\Delta_{\text{eff}} = J_0 (eV_{ac}/\hbar\Omega)\Delta$  [30,20].  $J_0$  is the zeroth order Bessel function of the first kind. Therefore, the resulting effective transmission  $T_{\text{eff}}(\epsilon)$  with the substitution  $\Delta \rightarrow \Delta_{\text{eff}}$  in Eq. (32) is

controllable via the driving parameters and even vanishes at zeros of the Bessel function.

The transformation (33) also affects the lead–well coupling. If we apply  $U_0(t)$  also to  $H_{\text{contacts}}$  and solve the Heisenberg equations for the lead and quantum-well operators in the wide-band limit, we can eventually extract the new fluctuation operator. For the left lead one finds

$$\begin{aligned} \eta_L(t) &= -\frac{i}{\hbar} \sum_q V_{Lq}^* \\ &\times \exp \left\{ -\frac{i}{\hbar} \epsilon_{Lq}(t - t_0) + \frac{ie}{\hbar\Omega} V_{ac} \sin(\Omega t) \right\} c_{Lq}(t_0), \end{aligned} \quad (35)$$

whereas  $\eta_R(t)$  remains unaffected. Now calculating the correlation function and time-averaging it over one driving period to neglect the  $\mathcal{T}$ -periodic contributions, the resulting expression assumes the form (25) but with the Fermi function of the left lead replaced by the effective electron distribution

$$f_{L,\text{eff}}(\epsilon) = \sum_{n=-\infty}^{\infty} J_n^2 \left( \frac{eV_{ac}}{\hbar\Omega} \right) f_L(\epsilon + n\hbar\Omega). \quad (36)$$

The squares of the  $n$ th-order Bessel function of the first kind in this expression weight those processes where an electron with energy  $\epsilon$  is transmitted from the left lead to the double-well system under the emission ( $n < 0$ ) or absorption ( $n > 0$ ) of  $|n|$  photons. The effective electron distribution exhibits steps at the energies  $\epsilon = \mu_L + n\hbar\Omega$  and is constant elsewhere.

With the effective quantities  $T_{\text{eff}}(\epsilon)$  and  $f_{L,\text{eff}}(\epsilon)$  the driven problem is ascribed for fast driving to a static one. Since  $T_{\text{eff}}(\epsilon)$  is sharply peaked around  $\epsilon = 0$  and  $f_R(0)$  and  $f_{L,\text{eff}}(0)$  are constant for finite voltage, the current in the high-frequency approximation results in

$$\bar{I} = \frac{e\Gamma}{4\hbar} \frac{\Delta_{\text{eff}}^2}{\Delta_{\text{eff}}^2 + (\Gamma/2)^2} \left[ 1 + \sum_{|n| \leq K(V)} J_n^2 \left( \frac{eV_{ac}}{\hbar\Omega} \right) \right] \quad (37)$$

applying the effective parameters to the current formula (1). Here  $K(V)$  is a shorthand notation for the integer part of  $e|V|/2\hbar\Omega$ .

In order to compare the transfer-matrix and the tight-binding approach, we have to ensure that the same physical situation is addressed. As a matching condition we compare the transmission  $T(\epsilon)$  in the time-independent case ( $V_{ac} = 0$ ). The level splitting energy  $2\Delta$  due to the central tunnel barrier is extracted from the resonance peaks of the doublet states computed within the transfer-matrix method. Solving for  $\Gamma$  in Eq. (32) with  $\epsilon = 0$  and  $T(0)$  and  $\Delta$  taken from the previous calculation, the corresponding lead–well coupling for the tight-binding system is determined.

#### 4. Coherent transport suppression

We now turn our attention to the coherent control of current. Tunnelling suppression in a closed, driven system is known for more than a decade. For example for a driven bistable potential, tunnelling breaks down at exact crossings of the quasi-energy spectrum, i.e., one observes the so-called *coherent destruction of tunnelling* [31,32]. Tunnelling suppression has been studied in a number of cases [22,33,34], but the investigation in a transport context, i.e., in an open system where an appropriate treatment of the leads is crucial, has received attention only recently [18,21].

Surveying the time-averaged current calculated numerically from the transfer-matrix and the tight-binding method plotted in Fig. 3, we observe current minima for distinct values of  $eV_{ac}/\hbar\Omega$  for frequencies in the microwave regime. The reason for the current suppressions becomes apparent by comparison with the high-frequency approximation, which exhibits minima close to those of the transfer-matrix and tight-binding curves. The current (37) vanishes whenever the ratio  $eV_{ac}/\hbar\Omega$  assumes a zero of the Bessel function  $J_0$ , i.e., for the values 2.405, 5.520, 8.654, ..., since then  $\Delta_{\text{eff}} \propto J_0^2 = 0$ . By varying the ratio between driving amplitude and frequency, we can thus tune the tunnelling between the two wells and thereby control the current [21]. For a frequency  $\Omega = 5\Delta/\hbar$ , the analytical expression (37) shows a remarkable agreement with the exact tight-binding result (30) for  $V_{ac} \lesssim V$ . The inset of Fig. 3 shows the minimum current at the first suppression decays as a function of the driving frequency  $\Omega$ . This is expected from the good agreement between the numerical results and the high-frequency approximation, because the approximation accounts for the first order term in a perturbative scheme in  $1/\Omega$  [18,21]. Higher order contributions are included in a numerically exact calculation,

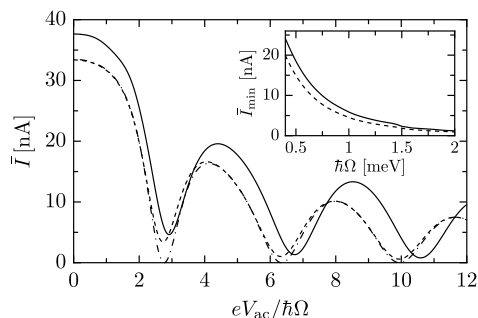


Fig. 3. Average current vs. driving amplitude obtained numerically from transfer-matrix (solid line) and tight-binding (dashed) methods. Also shown is the high-frequency approximation (dashed-dotted). The inset depicts the value of the first current minimum as a function of the driving frequency. Solid (transfer-matrix) and dashed (tight-binding) line decay approx. as  $1/\Omega$ . The chosen parameters are  $\hbar\Omega = 1.15$  meV,  $V = 6.0$  mV,  $\Gamma = 0.16$  meV and  $\Delta = 0.23$  meV. The corresponding parameters for the barriers are the same as those of Fig. 1.

which results in a non-vanishing current at the minima. A similar  $\Omega$ -dependence is observed also for the transfer-matrix formalism.

While the general shape and magnitude of the current are very similar for both models, there still appears a small difference in the location of the minima for the relatively low barriers chosen in Fig. 3. For a continuous potential, the current assumes minima at values of  $eV_{ac}/\hbar\Omega$  higher than those predicted by the tight-binding description. We can understand this shift by analysing, for given  $\Omega$ , the deviation  $\delta V = V_{\text{min}} - V_0$  of the driving amplitude  $V_{\text{min}}$  for which the current exhibits its first minimum. The amplitude  $V_0$  corresponds to the first zero of  $J_0$ . In Fig. 4 we plot  $\delta V$  as a function of  $\kappa d$ , where  $d = d_L = d_R$  and  $\kappa = [2m(V - \bar{\mu})/\hbar^2]^{1/2}$ , i.e.,  $\kappa d$  is the instanton action in units of  $\hbar$  and  $\exp(-2\kappa d)$  is the WKB transmission probability of the outer barriers in Fig. 1. Here  $V = V_L = V_R$  is the corresponding barrier height and  $\bar{\mu} = (\mu_L + \mu_R)/2$  denotes the average chemical potential representing approximately the mean energy of the resonance doublet.

If the width of the outer barriers is kept fixed,  $\delta V$  decreases for growing  $\kappa d$  because then the resonance energies are further away from the barrier edge. Therefore, the wave functions of the well states become more localised. This situation corresponds in the tight-binding picture to a lead–well coupling  $\Gamma$  that is almost energy independent and thus reproduces the wide-band limit. Furthermore, this argument is used to explain the smaller deviation observed with thinner barriers for the same  $\kappa d$ , since  $V_L$  is much larger in that case.

As can be seen by comparing data sets for different central barrier heights in Fig. 4, an increase of the height of the central barrier  $V_C$  reduces the level splitting  $2\Delta$ , that is, the overlap between the localised states in the left and right well in a tight-binding description. Thus the tight-binding and the transfer-matrix results converge as a function of the barrier height. Finally, it is important to note that varying any of the barriers affects the transmission properties of the whole heterostructure,

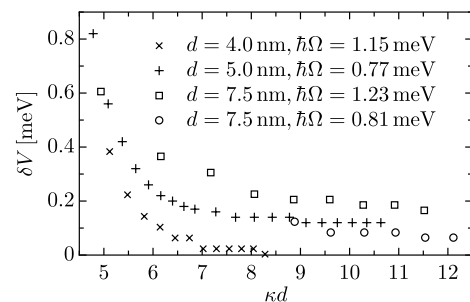


Fig. 4. Deviation of the driving amplitude for the first current minimum from the expected first zero of  $J_0$ ,  $V_0 = 2.405\hbar\Omega$ , for different barrier widths and heights. The parameters for the first three data sets are  $d_C = 15$  nm,  $\bar{\mu} = 12.0$  meV and  $V_C = 40$  meV, whereas for the last one (○), we chose  $\bar{\mu} = 13.3$  meV and  $V_C = 80$  meV.

in contrast to the tight-binding model, where the different coupling parameters can be controlled independently.

## 5. Conclusions

We have demonstrated that the dc current across a double-well heterostructure can be suppressed by the purely coherent influence of an oscillating gate voltage. We have used a transfer-matrix method as an exact approach to compute tunnelling currents through such a system. We compared these results to that obtained from a tight-binding Floquet description. In particular, we find that the current suppression is controlled by the ratio of the driving frequency and amplitude. This can be understood by exploring the high-frequency limit within the tight-binding formalism. In this perturbative scheme, the time-dependent system is mapped onto a static one with renormalised parameters, that is, with an effective hopping matrix element accounting for inter-well coupling and with an effective electron distribution for the attached left lead. Since the effective inter-well coupling depends on the ratio between driving amplitude and frequency, the transport properties of the double well can be adjusted through the driving parameters, with the effective behaviour ranging from transport through an almost open channel to a regime of rare tunnel events.

The results presented in this work strongly support the idea that transfer-matrix and tight-binding descriptions of quantum transport are equivalent provided the barriers are sufficiently high. In this case the lowest resonance states in the wells are rather localised and consequently the tight-binding description becomes accurate. For a proper choice of parameters, we find a good agreement between the exact transfer-matrix calculation and the results obtained within the tight-binding formalism. The study presented here shows that the coherent control of time-dependent electron transport can be investigated with current semiconductor nanotechnology.

## Acknowledgements

We thank Sébastien Camalet, Gert-Ludwig Ingold, and Jörg Lehmann for helpful discussions. Two of us (M.R. and F.S.) thank Mathias Wagner for introducing us to a numerical code based on [22]. This work has been supported through a joint Germany–Spain Acción Integrada (no. HA2003-0091). Financial support is also

acknowledged from MEC (Spain), Grant No. BFM2001-0172, Fundación Ramón Areces, and DFG (Germany), Graduiertenkolleg 283 and Sonderforschungsbereich 486. We also thank the Centro de Computación Científica (UAM) for technical and computational support.

## References

- [1] A.M. Kuznetsov, *Charge Transfer in Physics, Chemistry and Biology: Physical Mechanisms of Elementary Processes and an Introduction to the Theory*, Gordon and Breach, Luxembourg, 1995.
- [2] M. Bixon, J. Jortner (Eds.), *Advances in Chemical Physics*, Wiley, New York, 1999.
- [3] A. Nitzan, *Annu. Rev. Phys. Chem.* 52 (2001) 681.
- [4] P. Hänggi, M. Ratner, S. Yaliraki, *Chem. Phys.* 281 (2002) 111.
- [5] G. Cuniberti, G. Fagas, K. Richter (Eds.), *Molecular Electronics, Lecture Notes in Physics*, Springer, Berlin, 2005.
- [6] C. Beenakker, H. van Houten, *Sol. Stat. Phys.* 44 (1991) 1.
- [7] Y. Imry, *Introduction to Mesoscopic Physics – Mesoscopic Physics and Nanotechnology*, vol. 1, Oxford University Press, New York, 1997.
- [8] Ya.M. Blanter, M. Büttiker, *Phys. Rep.* 336 (2000) 1.
- [9] L. Esaki, R. Tsu, *IBM J. Res. Dev.* 14 (1970) 61.
- [10] R. Tsu, L. Esaki, *Appl. Phys. Lett.* 22 (1973) 562.
- [11] L.L. Chang, L. Esaki, R. Tsu, *Appl. Phys. Lett.* 24 (1974) 593.
- [12] T.C.L.G. Sollner, W.D. Goodhue, P.E. Tannenwald, C.D. Parker, D.D. Peck, *Appl. Phys. Lett.* 43 (1983) 588.
- [13] F. Capasso, S. Datta, *Phys. Today* 43 (1990) 74.
- [14] M. Grifoni, P. Hänggi, *Phys. Rep.* 304 (1998) 229.
- [15] G. Platero, R. Aguado, *Phys. Rep.* 395 (2004) 1.
- [16] S. Kohler, J. Lehmann, P. Hänggi, *Phys. Rep.* 406 (2005) 379.
- [17] P.K. Tien, J.P. Gordon, *Phys. Rev.* 129 (1963) 647.
- [18] S. Camalet, S. Kohler, P. Hänggi, *Phys. Rev. B* 70 (2004) 155326.
- [19] M. Wagner, *Phys. Rev. B* 49 (1994) 16544.
- [20] J. Lehmann, S. Camalet, S. Kohler, P. Hänggi, *Chem. Phys. Lett.* 368 (2003) 282.
- [21] S. Kohler, S. Camalet, M. Strass, J. Lehmann, G.-L. Ingold, P. Hänggi, *Chem. Phys.* 296 (2004) 243.
- [22] M. Wagner, *Phys. Rev. A* 51 (1995) 798.
- [23] R. Landauer, *IBM J. Res. Dev.* 1 (1957) 223.
- [24] M. Wagner, F. Sols, *Phys. Rev. Lett.* 83 (1999) 4377.
- [25] H. Sambe, *Phys. Rev. A* 7 (1973) 2203.
- [26] J.H. Shirley, *Phys. Rev.* 138 (1965) B979.
- [27] M. Wagner, H. Mizuta, *Phys. Rev. B* 48 (1993) 14393.
- [28] S. Datta, *Electronic Transport in Mesoscopic Systems*, Cambridge University Press, Cambridge, 1995.
- [29] D.S. Fisher, P.A. Lee, *Phys. Rev. B* 23 (1981) 6851.
- [30] F. Großmann, P. Hänggi, *Europhys. Lett.* 18 (1992) 571.
- [31] F. Grossmann, T. Dittrich, P. Jung, P. Hänggi, *Phys. Rev. Lett.* 67 (1991) 516.
- [32] F. Großmann, P. Jung, T. Dittrich, P. Hänggi, *Z. Phys. B* 84 (1991) 315.
- [33] M. Holthaus, *Phys. Rev. Lett.* 69 (1992) 351.
- [34] C.E. Creffield, G. Platero, *Phys. Rev. B* 65 (2002) 113304.